

On the Origin of Shrimpluminescence

Tyler C. Sterling*

(Dated: January 13, 2022)

[illegible]

I. INTRODUCTION

Snapping shrimp, like our cute friend in Fig. 1 (left), have long been known to produce cavitating bubbles by *snapping* their claws [1; 2; 3]. They have a strong appendage (the *dactyl*) in their claw [Fig. 1 (center)] that is used to create a very high-velocity jet of water. The low pressure region in the jet’s wake forms a bubble [Fig. 1 (right)] that, among other things, produces an exceptionally loud noise when it collapses. The sound (i.e. the pressure wave) produced by even a *single* shrimp’s snap is detectable over a mile away [4]. The noise produced by groups of shrimp is so intense that the U.S. Navy used them as “sonar-camouflage” in the Pacific ocean during World War II [1].

The shrimp were not patriots helping the war-effort, however; they snapped for food. The shock-wave produced by the cavitating bubble is used to stun and even kill prey [1]. If the shrimp’s prey had very¹ sensitive eyes (and also were not dead) they might notice a flash of light is also produced through an effect referred to as “shrimploluminescence” in the case of the pistol shrimp [2], but more generally known as *sonoluminescence*.

Sonoluminescence (SL) is more precisely defined as the process by which a “driven gas bubble collapses so strongly that the energy focusing at collapse leads to light emission” [5]. SL comes in two forms: (i) single-bubble sonoluminescence and (ii) multi-bubble sonoluminescence. The distinction is self-explanatory: multi-bubble sonoluminescence (MBSL) consists of “the simultaneous creation and destruction of many separate, individual cavitation bubbles” [5; 6], whereas in single-bubble sonoluminescence (SBSL), rather obviously, only a single bubble is present [7]. The discovery of MBSL predates SBSL by ~ 60 years but due to the more-or-less random and fleeting nature of the bubbles, SL in general wasn’t well studied until the early 1990’s when it was discovered that single bubbles could be created and

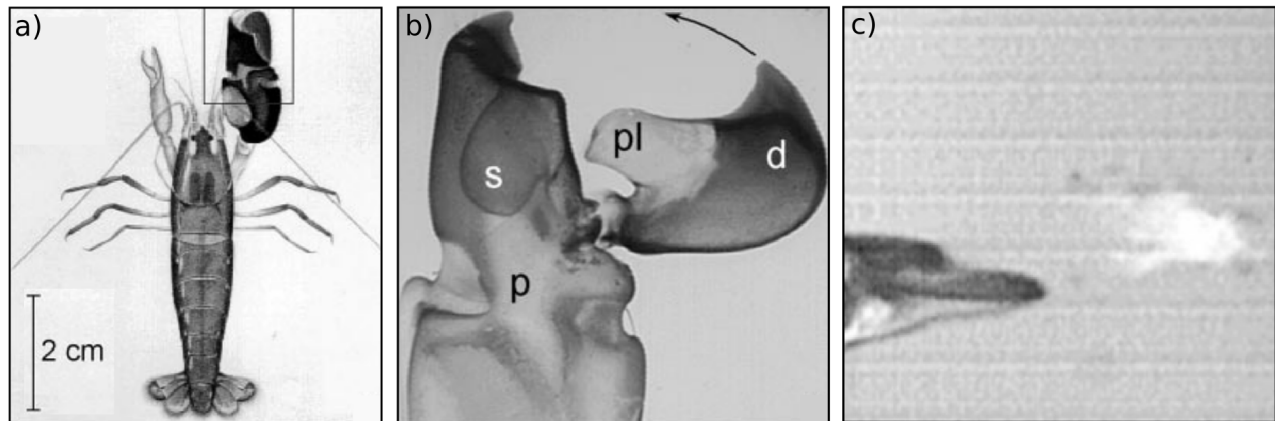


FIG. 1 (left) Snapping shrimp (*Alpheus heterochaelis*). (center) Blown-up view of the shrimp's claw. The *plunger* (pl) on the *dactyl* (d) rapidly enters the *socket* (s), ejecting a high-velocity jet of water. A time near the bubble collapse is shown on the right. The light emission is too dim to be seen by the naked eye. Adapted from refs. [1] and [2].

* ty.sterling@colorado.edu

¹ We stress *very*: shrimpoluminescence is too weak to be seen by the naked-eye.

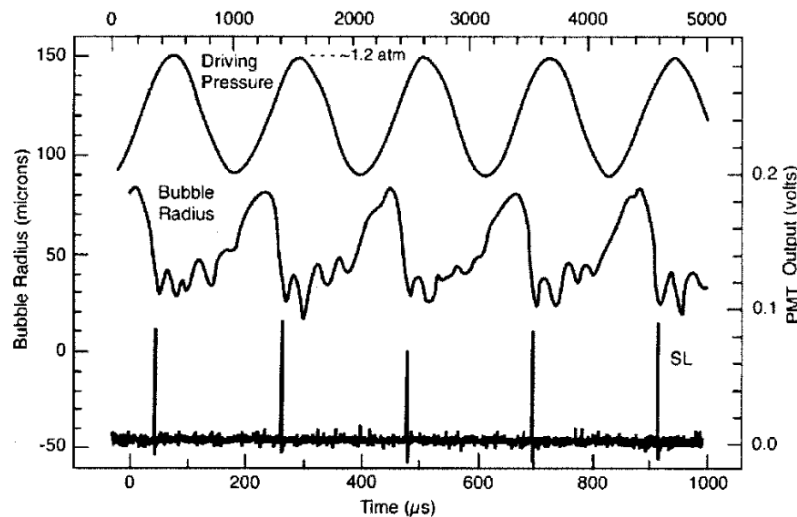


FIG. 2 [5; 6]

periodically driven to produce light with very high precision [5; 6; 7; 8]. In SBSL, emission from a single bubble is not complicated from multiple scattering (off other bubbles), volumetric-light emission from the bubble cloud, etc. Similarly, the bubble is not perturbed by interaction with other bubbles and, due to its tiny size, by interaction with the container walls. As a result, the theory is greatly simplified compared to MBSL. It is not an exaggeration to say that nearly all theoretical and experimental progress to explain SL has been made using SBSL, with some authors even calling it “the hydrogen atom of SL” [6; 9].

Studying SBSL, while offering advantages, also comes with complications. Due to the tiny volume of the bubble, directly measuring the temperature or pressure *inside* the bubble is practically impossible [10]. Still, the discovery of SBSL created a rush of effort to explain the phenomena with arguments ranging from the simplest models² to more exotic explanations based on quantum field theory [11; 12; 13]. Over time, the *phase-space* of SBSL has been refined: SBSL only occurs for a narrow range of driving pressures and for a particular combination of host-liquid and gas content in the bubble. The mapping of the phase-space of SBSL is a very rich subject and merits a review in itself (several exist [5; 14]). We will not pursue this; our goal in this paper is to explain *shrimpluminescence* so we will mainly focus on SBSL as it occurs in *water* containing *air bubbles*, though occasionally we will comment on SBSL in other fluids.

Let us now sketch the SBSL process a little more precisely. An air bubble is trapped at the center of an acoustically driven flask containing a fluid. The pressure wave in the fluid, shown as a function of time in Fig. 2, drives the expansion and contraction of the bubble and, in turn, the dynamics of the gas in the bubble responds to the bubble’s oscillations. Within the phase-space relevant to SBSL, we get the very complicated non-linear response of the bubble’s radius as shown in Fig. 2. Let’s see how these dynamics lead to SBSL.

First, as the pressure decreases and becomes negative, the bubble expands gradually: surface tension and the negative pressure in the bubble tend to slow this down. Eventually the pressure is increasing again. Once it becomes positive, the bubble violently collapses to its minimum radius: during compression, the negative pressure in the bubble is very large and works with the driving pressure to rapidly accelerate the bubble’s wall. Since the collapse is so quick, the bubble’s contents are adiabatically compressed, resulting in very large temperature and pressure in the bubble. If everything is just right, the temperature and pressure are large enough for a burst of light to be produced as shown by the bottom curve in Fig. 2. After the collapse, there is a period of *after-bouncing* that continues until the pressure is negative again.

It turns out that the light pulse is very short (only $\sim 0.003\%$ of the bubble’s cycle [10]) and its spectrum depends sensitively on both the mechanical and chemical properties of the host-liquid and gas in the bubble, as well as the driving pressure and frequency [5; 10]. The mechanical properties determine the pressure and temperature inside the bubble which in turn control chemical reactions: all of these data are used to explain the light emission. For extreme

² There are far too many to try list here and we will not be interested in the vast majority of early models which are now irrelevant. References to these can be found in Gaitan [8] and Brenner et al. [5].

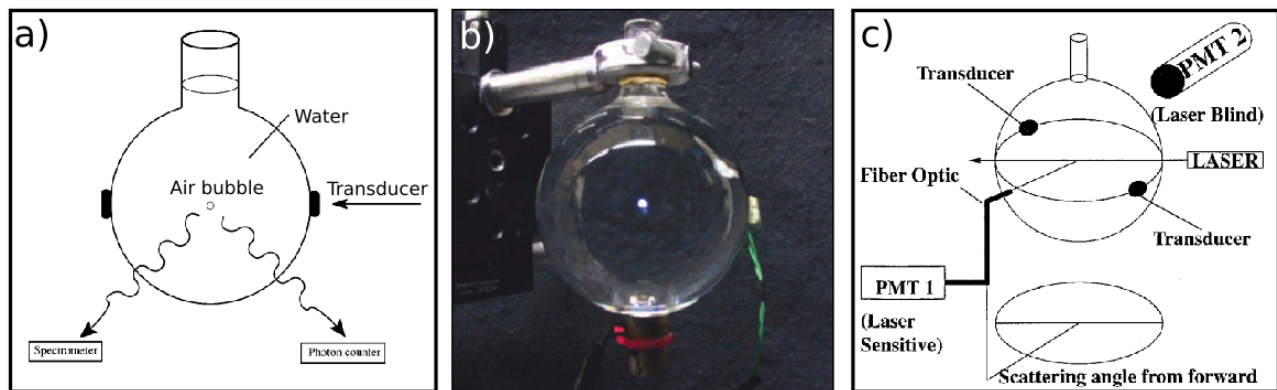


FIG. 3 (a) Schematic of a spherical acoustic levitation cell. The piezoelectric transducers that drive the bubble trapped in the flask are labeled in the diagram. (b) Photograph of the same. Here, the fluid is aqueous H_2SO_4 instead of water. A sonoluminescing bubble is clearly visible in the center of the flask. The photo was taken in a fully lit room with exposure time 2 s. (c) Schematic of a Mie scattering experimental setup. A similar acoustic levitation cell as (a) is shown with an added laser source and photomultiplier tubes (PMT) to analyze the scattered and emitted light. (a), (b), and (c) are from refs. [5], [10], and [22] respectively.

enough conditions in the bubble, which occur only briefly, molecular dissociation and recombination, atomic/excited-state transitions, and electron-ion/electron-neutral atom bremsstrahlung are possible [10; 15; 16; 17; 18; 19]. These are now known to be the processes which emit light [9; 14].

Our goal in this paper is to present the simplest theory needed to understand *shrimpluminescence*, though we will actually concentrate on the related physics of a bubble undergoing SBSL in the lab as it is apparently simpler to create and characterize SBSL without involving shrimp³. Firstly, we will look at the problem of the fluid containing the bubble; we will derive the equations of motion for the bubble's wall. Next, we will use our results for the bubble's wall to understand the dynamics of the gas trapped in the bubble. The result of this will turn out to be an estimate of the *temperature* and *pressure* in the bubble. We will then look at theories presenting the origin of light from the very hot contents of the bubble. For relatively mild conditions inside the bubble, most light emission occurs during molecular dissociation processes [1]. These are the conditions in e.g. weakly driven 85% H_2SO_4 . In water, the pressure in the bubble is considerably higher and most light emission is due the electron-ion and electron-neutral atom bremsstrahlung which occur at higher temperatures [10; 15; 18]. Recalling that we want to understand SBSL in water, we will mainly focus on these latter processes. Moreover, throughout the course of our journey, we will stick to the simplest results that still contain the essential physics we need. Connections to more advanced treatments, and their implications, are provided for completeness.

A. Historical Overview

MBSL was discovered by accident in 1933 by Marinesco and Trillat [20] and was subsequently characterized by Frenzel and Schultes [21]⁴ Marinesco et al. were trying to accelerate photo development by *insonating* developing fluid. They discovered that a photosensitive plate immersed in the insonated fluid became “foggy,” which they attributed to exposure to light. Shortly after, Frenzel et al. repeated the experiment and confirmed that the insonated fluid emits light in the form of a faintly glowing cloud of bubbles.

This result was not particularly surprising to the community since it had been known for a while that cavitating bubbles, e.g. those generated by the sound field, could do tremendous damage to ship's propellers⁵. The discovery's impact is concisely summarized by Brenner: “if the cloud [of cavitating bubbles] collapses violently enough to break molecular bonds in a solid, why should it *not* emit photons” [5]. In fact, cavitating bubbles had been of interest to engineers working on fluid mechanics for a while. The discovery of cavitation is credited to Euler (as early as

³ For example, convincing the shrimp to snap requires tickling them [1; 2; 9]. Besides notable exceptions [3], practically all work to study SL has not involved shrimp.

⁴ Neither the paper due to Marinesco et al. nor the one due to Frenzel et al. can be found by the author; in any case he can't read French or German so having the papers wouldn't be much use. As such, the story of how the effect was discovered is taken from more recent sources whose authors hopefully could read French and German [5; 6; 8]

⁵ A more modern example could be my van's oil pump, which is in need of replacing.

1754) who hypothesized that if the velocity in a fluid was large enough, negative pressures could become so large as to “break the fluid” [7; 23]. Cavitation was confirmed to exist (and named “cavitation”) in 1895 by engineers studying the failure of a British Navy ship’s propeller [23]. Shortly after, Lord Rayleigh wrote down and solved the differential equation for a vapor filled cavity collapsing in water (the so-called Rayleigh equation), giving the first rigorous theoretical treatment of cavitation [24; 25]. Rayleigh found that, for a bubble at a lower pressure than the surrounding fluid (and both pressures held constant), the bubble wall diverges during collapse. The theory has been refined considerably since then [5; 25; 25; 26; 27; 28] and we will devote a large portion of this paper to this subject. Still, very little information was accessible about the light emission until the 1990’s when stable ⁶, single bubbles could be created and driven to emit light [6; 7; 8]. With this discovery, serious interest took root.

SBSL, unlike previous studies on MBSL, allowed very precise control and measurement of the SL process. With unprecedented experimental control, many discrepancies in previous assumptions about SL were discovered. Experiments measuring the duration of the light pulse found that it was orders of magnitude smaller than the time in which the bubble was compressed to its smallest radius [28; 29]. This discovery implied that SL was nearly decoupled from the bubble’s dynamics. New models were proposed based on *converging shock waves* at the bubble’s center with estimates of the temperature at the center of bubbles $\sim 10^8$ K [30; 31]. At the same time, experimentalists fit the bubble’s light emission spectra as a *black body emitter* and concluded that the temperature in the bubble was at least 25,000 K [32].

These very high estimates for the temperature in the bubbles led to a spark of interest more broadly: if the temperature in the bubble were really that large, then it should be possible for nuclear *fusion* to occur []. An action movie featuring Keanu Reeves was even made with this at the center of the plot ⁷. In the early 2000’s, several papers were even published claiming that stable nuclear fusion was possible in the lab using a method based on SBSL []. Unfortunately these results turned out to be fraudulent []. Shortly after this fiasco, evidenced emerged that there are shape instabilities in the bubbles dynamics indicating that the converging shock-wave hypothesis is probably not right. This severely reduced the estimates for the temperature to $\sim 10,000$ K, ruling out the possibility of fusion occurring at all []. Moreover, it was shown that the light is most likely emitted from the *bulk* of the bubble as opposed to its surface, making fits to a black body spectrum (i.e. surface emission) incorrect []. Current estimates for the temperature, which we will study in the rest of this paper, put the center of a sonoluminescing bubble at $10,000 - 30,000$ K [10; 14; 15; 16; 17; 18].

II. BUBBLE DYNAMICS

In this section, we will present the theory needed to model and understand the dynamics of a bubble undergoing SBSL. We will split this into parts. Firstly, we will derive the equations of motion for the bubble’s wall. Nextly, we will review some important experimental developments that we will then use to argue for a simple model for the dynamics of the gas in the bubble. Lastly, we will compare results of a simulated bubble to experimental data. The connection to experiment will be what allows us to calculate the temperature in real bubbles.

A. The Bubble Wall

As it turns out, the dynamics of the bubble in SBSL (regardless of the light emission) are quite well described both qualitatively and *quantitatively* by the classical theory of bubble dynamics [5; 10; 14; 25; 26; 33; 34]. This isn’t particularly surprising since the light emission and bubble collapse occur at different timescales (the duration of maximum compression’s is $\sim 0.003\%$ of the bubble’s period) [5; 10; 25; 26; 33]. The starting point for any theory of the bubble dynamics is Rayleigh’s original work [24], now expounded upon by many others. The most widely known modern work is that of Plesset [25; 33; 35], resulting in the so called “the Rayleigh-Plesset” (RP) equation. The derivation assumes the host liquid is incompressible, ultimately resulting in us neglecting the effects of sound radiated by the bubble. Corrections exist that improve upon the RP equation in various ways and we will discuss these below []. However, for brevity’s sake, we will only derive the RP equation here and merely quote the others as they are very similar in form to the RP equation. The field of *bubble dynamics* is quite mature and attempting to review it here would be out of scope of this paper; instead, the reader is referred to numerous books and reviews [5; 14; 26; 33].

⁶ *Stable* is compared with *transient* when discussing cavitation. A stable bubble persists through multiple cycles of cavitation, oscillating non-linearly around an equilibrium size. Transient bubbles appear and then collapse to disappear

⁷ It is called *Chain Reaction* and I am unwilling to watch it.

The RP equation can be deduced from the *Navier-Stokes* (NS) equations⁸ [5; 10; 14; 25; 26; 33]. The NS equations for a compressible fluid are

$$\begin{aligned} \rho \frac{d\mathbf{u}}{dt} &= \rho [\partial_t \mathbf{u} + (\mathbf{u} \cdot \nabla) \mathbf{u}] = -\nabla p + \eta \nabla (\nabla \cdot \mathbf{u}) + \mu \nabla^2 \mathbf{u} + \mathbf{f}_B \\ \partial_t \rho + \nabla \cdot (\rho \mathbf{u}) &= 0. \end{aligned} \quad (1)$$

Here, $\mathbf{u}(\mathbf{x}, t)$ is the velocity of a fluid parcel at position \mathbf{x} at time t , $\rho(\mathbf{x}, t)$ is the fluid's density, p is the pressure, $\eta \equiv (\xi + \frac{2}{3}\mu)$ is the *bulk* viscosity with μ the *shear* viscosity, and \mathbf{f}_B are *body* forces (e.g. gravity, electrostatic forces) which are usually from external sources and will be assumed negligible from here on. The subscripts on ∂ denote what derivative is being taken and ∇ and ∇^2 have their usual meanings. The first equation is *conservation of momentum* for the fluid, i.e. Newton's 2nd law; the second equation is *mass conservation*. The total-derivative of a moving fluid $\frac{d}{dt} \equiv D_t$ is sometimes called the *material derivative*. In the case of velocity $D_t \mathbf{u}$ is the *acceleration* of the fluid. It records not only explicit time dependence of the fluid's velocity $\partial_t \mathbf{u}$ but also how the fluid's velocity varies *in space* as it moves past us: $(\mathbf{u} \cdot \nabla) \mathbf{u}$. The pressure term on the right hand side is to be understood as forces from the *elastic* energy. On the other hand, the terms $\sim \mathbf{u}$ are viscous (damping) terms that tend to make the velocity field spatially uniform: they vanish when the (spatial) derivatives of the velocity vanish. The bulk-viscosity term $\sim \eta$ damps radial changes in the fluids velocity (e.g. dilation/contraction) while the shear-viscosity term $\sim \mu$ resists shearing.

Solving eqs. 1 is an intractable problem. To make progress, we will make some drastic approximations that are more-or-less valid for our problem. Firstly, we will assume irrotational flow (i.e. $\nabla \times \mathbf{u} \equiv 0$) so that there is only radial motion in the liquid (i.e. $\mathbf{u} = u\mathbf{r}$). Note that, since the flow is assumed irrotational, we can represent the velocity as the gradient of a scalar function: $u\mathbf{r} = \partial_r \phi \mathbf{r}$ [36]. This amounts to assuming that the bubble is always spherical which seems like a rather drastic approximation but has been validated experimentally in many cases []. The fact that the bubble tends to remain spherical can be understood by accounting for surface-tension at the liquid-bubble interface [26].

Nextly, we assume that the viscous terms are negligible in the bulk dynamics of the liquid. For (relatively) low viscosity fluids such as water which is also nearly incompressible, this is an accurate approximation and is widely used [5; 25; 26; 33]. We will account, to some extent, for viscosity later when looking at the bubble-liquid interface. Moreover, we are assuming that the flow is *isentropic*, i.e. that it is reversible (no damping) and that no heat is exchanged between fluid parcels. We will further assume that the liquid is isothermal, i.e. its temperature is constant (in space). Then pressure p is determined from an instantaneous equation-of-state $p = p(\rho, T)$. In the case of SBSL, this is valid since the bubble makes up a *tiny* fraction of the total volume and, as we will later see, heat-transport across the liquid-bubble interfacing is usually neglected anyway (i.e. the bubble is compressed adiabatically in the thermodynamic sense⁹).

Lastly, related to the fact that the bubble is tiny, we assume that the extent of the liquid is so large compared to the bubble that we may consider the dynamics of the liquid as if there were no bubble present; similarly, we consider the dynamics of a bubble in an infinite, isotropic medium. Of course the bubble-liquid interface enters both systems as a boundary condition [33].

With these simplifying assumptions (and a vector identity¹⁰) we rewrite eqs. 1 as a system of 1 + 1 dimensional partial differential equations:

$$\begin{aligned} \partial_r \left[\partial_t \phi + \frac{1}{2} (\partial_r \phi)^2 \right] &= -\frac{1}{\rho} \partial_r p \\ \partial_t \rho + \partial_r \phi \partial_r \rho + \rho \partial_r^2 \phi &= 0. \end{aligned} \quad (2)$$

We can integrate the first equation above using the fact that the compressibility is negligible to move the density through the integration [37]

$$\int_{r_\infty}^r \frac{\partial}{\partial r'} \left[\frac{\partial \phi}{\partial t} + \frac{1}{2} \left(\frac{\partial \phi}{\partial r'} \right)^2 \right] dr' = -\frac{1}{\rho} \int_{r_\infty}^r \frac{\partial p}{\partial r'} dr'. \quad (3)$$

⁸ The NS equations are derived in the appendix

⁹ According to Wikipedia, *adiabatic* means *fast* in thermodynamics lingo. This is relevant to us since we are claiming the bubble wall moves so quickly that it is compressed to its maximum pressure before any heat can flow out. On the other hand, the mechanics lingo implies *adiabatic* to mean *slow*. This is, e.g. the adiabatic theorem in quantum mechanics: a perturbation acts so slowly that the system is in its ground state at all times.

¹⁰ $(\nabla \cdot \mathbf{u}) \mathbf{u} = \frac{1}{2} \nabla(u^2) - \mathbf{u} \times (\nabla \times \mathbf{u})$

On the left side, we take the velocity to vanish at infinity. On the right side, we assume that only the static and unperturbed pressures, p_∞ and $P(t)$ respectively, are relevant so that [26; 33; 37]

$$\partial_t \phi + \frac{1}{2} (\partial_r \phi)^2 = \frac{(p_\infty + P(t)) - p(t, r)}{\rho}. \quad (4)$$

Eq. 4 gives the pressure at coordinate (r, t) in terms of the velocity of the fluid, the density, and the applied pressure.

Now, let us assume that the velocity potential satisfies a wave equation $\nabla^2 \phi - \frac{1}{c^2} \partial_t^2 \phi = 0$ ¹¹ with c the speed of sound in the fluid. Again, we use incompressibility by recalling that for an incompressible fluid $c \rightarrow \infty$ which implies $\nabla^2 \phi = 0$ ¹². In this case, we can ignore retardation effects and, remembering that we have spherical symmetry, write the solution of $\nabla^2 \phi$ as

$$\phi = \frac{\psi(t)}{r} \quad (5)$$

with ψ the time-dependent coefficient. We now use the boundary condition for the velocity at the bubble wall, $u(R) \equiv \dot{R}$ with R the bubble radius, to determine ψ :

$$\dot{R} = -\frac{\psi}{R^2} \Rightarrow \psi = -R^2 \dot{R}. \quad (6)$$

Thus, we find $\phi(r, t) = -\frac{R^2 \dot{R}}{r}$. Plugging this into the left hand side of eq. 4 and evaluating at the bubble wall, $r \equiv R$

$$\begin{aligned} \partial_t \phi|_{r=R} &= -2\dot{R}^2 - R\ddot{R} \\ \partial_r \phi|_{r=R} &= \dot{R} \equiv u(R) \end{aligned} \quad (7)$$

Finally, sticking all this together, we arrive at the Rayleigh-Plesset equation [25; 26; 33; 35; 37]

$$R\ddot{R} + \frac{3}{2}\dot{R}^2 = \frac{p_B(t) - (p_\infty + P(t))}{\rho} \quad (8)$$

with $p_B \equiv p(r = R, t)$ the pressure in the fluid at the bubble wall. Evaluated beyond the bubble wall, $r > R$, eq. 8 gives the pressure radiated by the fluctuating bubble. Some comments are in order. The combination $p_\infty + P(t)$ is the *ambient* pressure [26; 33] which gives the pressure in the fluid in the absence of the bubble. The left hand side of eq. 8 may be regarded as the kinetic energy (density). The right hand side is the change in enthalpy (density) due to the fluctuating bubble, i.e. the dynamics of the bubble given on the left hand side are determined by the enthalpy in the fluid due to the bubble's motion. In deriving this equation, we have assumed that the speed of propagation in the fluid is infinite. In reality, this is not true but this approximation will be very good close to the bubble (in the *near-field*) where retardation effects are negligible anyway. In a similar way, we have assumed that the energy in the fluid due to distorting its volume is negligible. This approximation will be accurate near the bubble as well since the kinetic energy in this region will dominate [26].

We can refine eq. 8 a little further. Since the motion in the fluid is purely radial, we expect the only relevant stresses to be normal to the bubble wall. Let's denote the radial stress in the liquid at some point r by $s_r(r) = -p(r, t) + 2\eta\partial_r u$. Recall, η is the fluid viscosity from earlier. Using conservation of mass and momentum, and our expression above for the velocity, we can equate the normal stresses in the fluid to those in the bubble:

$$s_r(R) = -p_B - 4\frac{\eta\dot{R}}{R} = -p_g + 2\frac{\sigma}{R} \quad (9)$$

where p_g is the pressure in the gas and σ is the surface tension. Solving for $p_B(t)$, we have the relation [5; 26; 33]

$$p_B(t) = p_g(t) - \frac{1}{R} (2\sigma + 4\eta\dot{R}). \quad (10)$$

¹¹ This doesn't come from thin air. We could write the r.h.s. of eq. 4 as the enthalpy, $h \equiv \int \frac{dp}{\rho}$, and similarly introduce $dh = \frac{dp}{\rho}$ in the first line of eq. 2. Eliminating h between the two and dropping small terms $\sim \frac{u}{c}$, we arrive at the homogeneous wave equation [5; 26; 37].

¹² For our problem, it is true that $(\frac{1}{c^2} \partial_t^2 \phi) / \nabla^2 \phi \sim \left(\frac{R}{\lambda}\right)^2 \ll 1$, i.e. the long wave-length approximation is accurate [26; 33; 37].

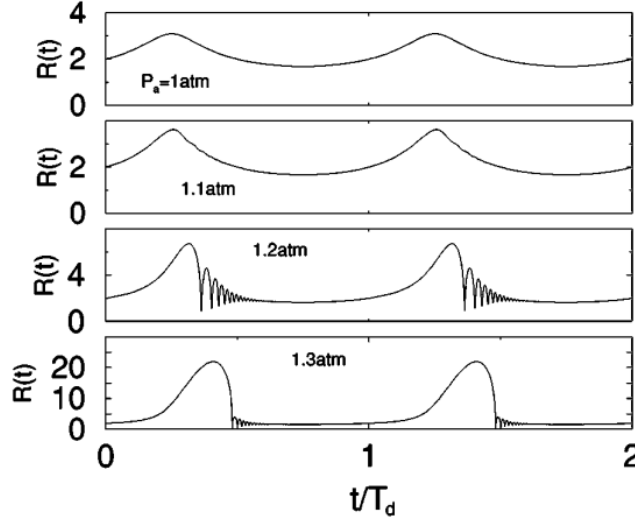


FIG. 4 [5]

Note that in deriving the equations 2 we neglected the viscosity terms. This was valid since only combinations of viscosity and compressibility $\nabla \cdot \mathbf{u}$ appeared, both of which are assumed small. Here, however, we opt to keep the viscosity terms coupling the bubble wall to the fluid. With this, we can rewrite the RP equation as

$$R\ddot{R} + \frac{3}{2}\dot{R}^2 = \frac{1}{\rho} \left[\Delta p(t) - \frac{1}{R} (2\sigma + 4\eta\dot{R}) - P(t) \right] \quad (11)$$

with $\Delta p = p_g(t) - p_\infty$ the deviation of the pressure inside the bubble from the static pressure. With the above assumption that the compression is adiabatic, the conditions inside the bubble are decoupled from the liquid (besides the coupling through the RP equation) and we may regard $p_g(t)$ in the bubble as a given quantity to be determined from an equation of state. Recall $P(t)$ is the time-dependent part of the pressure in the absence of the bubble: we may regard this as an external pressure from e.g. a driving stress. This will be from the transducers driving the acoustic levitation cell.

Eq. 11 is the equation of motion for a driven spherical bubble in an infinite, incompressible fluid. It is worth briefly summarizing this all again. On the left hand side, R is the radius of the bubble, \dot{R} is the velocity of the bubble's radius i.e. the velocity of the *bubble wall*, and \ddot{R} is the bubble wall's acceleration. On the right hand side, ρ is the (constant) density of the fluid. $\Delta p(t) = p_g(t) - p_\infty$ is the deviation of the gas pressure in the bubble, $p_g(t)$, from the static fluid pressure at infinite distance, p_∞ . $p_g(t)$ is evaluated at the bubble wall. In the second term, the $\sim \sigma$ part gives the restoring force from surface tension stresses while the $\sim \eta$ term is due to the fluid viscous stresses: σ and η are the surface tension and viscosity coefficients respectively. The last term on the right, $P(t)$, is the *external pressure*. For problems relevant to SBSL, the driving pressure, $P(t)$ in the RP equations, is an acoustic plane wave. Keller and coworkers showed that the modification required to the RP equations result in the replacement $P(t) \rightarrow P_0 \sin(\omega t)$ [38]. If we linearize in the bubble's radius $R(t) \approx R_0 (1 + x(t))$ with $x(t) \ll 1$, we can derive a forced harmonic oscillator equation for $x(t)$ [14; 34]. However, the low driving amplitude regime where this method is valid is irrelevant to SBSL so we won't pursue it here.

Let us briefly digress to discuss retardation effects. If we had not assumed incompressibility, our solution would include a term arising from the sound radiation from the bubble itself. There are practical issues with this solution however; it is *third* order in time and has unphysical, exponentially diverging solutions [5; 26; 33; 39]. Both issues are solved by imposing boundary conditions on the \ddot{R} term. The method for doing so is also challenging and apparently no unique way to do it exists [33; 40; 41]. Instead, there is a whole family of solutions that can be derived; different variations of the improved RP equation, which are collectively referred to as "Rayleigh-Plesset equations" are derived by neglecting different terms in the full compressible solution. We will discuss this again below.

The RP equation (eq. 11) is pretty but its analytical solution intractable. Direct solutions of the RP equation or its variants are done numerically using e.g. the Euler method [14; 42]. It is no great challenge computationally. For now, let's see what we else we can understand from this analytically by making some more approximations. If we look at the interval where the bubble wall's velocity is very large, called *The Rayleigh Collapse*, the \dot{R}^2 term will be

much larger than the right hand side of eq. 11 and we may neglect it. [5; 24; 26; 35]. Rayleigh looked at the same problem, i.e. a cavitating *void* in water, by replacing $p_0 \rightarrow 0$ [5; 24]:

$$R\ddot{R} + \frac{3}{2}\dot{R}^2 = 0 \quad (12)$$

and found the solution to be $R(t) \sim (t_* - t)^{2/5}$ [5], with t_* the time of collapse. The *velocity*, $\dot{R} \sim (t_* - t)^{-3/5}$ diverges as the bubble collapses. This observation is what lead to Rayleigh's argument for the origin of cavitation damage to ship's propellers. Yasui gave a rather elegant heuristic explanation for the origin of *cavitation* in a fluid that is worth stating here [14]. Consider the mass flowing through concentric shells around a bubble, $4\pi R_i^2 v_i \rho$. For a source free field, we require that neighboring shells satisfy conservation of mass: $4\pi R_1^2 v_1 = 4\pi R_2^2 v_2$. For $R_2 > R_1$, we see that $v_1/v_2 = (R_2/R_1)^2$. The velocity for a smaller radius is always larger, diverging towards the origin.

In reality, the bubble's velocity does not become infinite and, in the case of *stable* SBSL, the radius remains finite at all times. In the full RP equation (eq. 8) the only term capable of compensating the bubble wall's motion is the diverging pressure inside the bubble itself [5]. Applying the same analysis to the family of solutions derived when including the bubble's sound radiation, it turns out that the most important term for slowing the bubble wall's diverging velocity is $\propto \dot{p}_g$. Keeping only this term, we arrive at the most popular variant of the RP equation [27; 43]:

$$R\ddot{R} + \frac{3}{2}\dot{R}^2 = \frac{1}{\rho} \left[\Delta p(t) - \frac{1}{R} (2\sigma + 4\eta\dot{R}) - P(t) + \frac{R}{c} \dot{p}_g \right]. \quad (13)$$

This equation is only slightly more complicated than the RP equation (eq. 11), the only change being the added term $\propto \dot{p}_g$ which is determined from solving the decoupled problem of the gas inside the bubble. Eq. 13 is usually solved numerically; we will look at results of numerical solutions later when talking about experiments. For now, we note that the observed error between this equation and experiment is only significant in the interval during bubble collapse and even still, results of solving this equation are quantitatively in good agreement with measurements of the bubble's radius [5].

B. The Bubble's Interior

The theoretical progress on the bubble's interior since the discovery of SBSL in the late 1990's [7] follows two paths [5; 10; 14]: (i) model calculations based on the RP equations and an equation of state for the pressure (from which we may calculate the temperature) are used to try to reproduce the easily measurable dynamics of the bubble. (ii) We can model the light emission itself and compare our calculation to spectroscopic measurements of SBSL []. Obviously these are related topics, but the distinction in the context of SBSL is important as we will now see.

Most early progress on the bubble's interior depended on the former method: if we predict the right dynamics, then we might know the correct pressure and temperature in the bubble. These data are then used to try to describe the light emission []. This was preferred to studying the emitted spectra directly as careful measurements resulted in an almost featureless spectrum that could not be explained []. Calculating the dynamics of the bubble's wall from the RP equations (eq. 11 or eq. 13) requires the pressure inside the bubble as input. We would like to find a suitable form for $\Delta p(t) \sim p_g(t)$ in the RP equations that reproduces the measured radius-time curve $R(t)$ for a stable cavitating bubble. It turns out that this is a very complicated problem: gas diffusion and rectification (one-directional diffusion) between the bubble and liquid vary the number of particles present and, to make things worse, the conditions inside the bubble facilitate chemical reactions between the air and water-vapor changing the properties of gas dynamically [5]. Brenner et. al elegantly summarized the significance of this problem [5]: "one of the exciting features of modern research on SBSL is that it is a testing ground for how well mathematical models can deal with such a complicated situation"

The other method to understand the bubble's interior is its light spectrum. For the first decade or so, SBSL experiments were done using partially degassed¹³ water as the liquid medium [5; 7; 10]. Careful measurements of the emission from SBSL in water resulted in an almost featureless spectrum []. Early attempts were made to fit this as black-body radiation resulting in *huge* temperature estimates, e.g. 10^8 K []. It was later discovered that SBSL is volume emission, indicating that black-body radiation is not valid [44; 45]. Little progress was made on this front for quite some time [5]. The utility of analyzing the light spectrum of SBSL in water is succinctly described by Suslick

¹³ Degassing lowers the ambient pressure, making it easier for bubbles to form.

[10]: “because of the inherent ambiguity associated with the analysis of featureless spectra of unknown origin, a more rigorous explanation is unlikely to be generated”.

Some attempts were made to measure SBSL using non-aqueous host liquids e.g. alcohols, silicone oils [43; 46], but experiments with air bubbles were not very successful [43]. Eventually, different gases were tried in water. Recall, air is $\sim 80\%$ N_2 , $\sim 20\%$ O_2 , and $\sim 1\%$ Ar. Considering the relatively large content of O_2 and N_2 , degassed water *regassed* with N_2 or O_2 or a mixture were checked first and found not to produce SBSL [47]. What was discovered was that a small amount of *noble gas* was required for SBSL to occur [5; 43; 47]. A result of this work was the *argon rectification hypothesis* [5; 10; 14; 48]. The hypothesis claims that all species in the air inside the bubble besides argon are gradually ejected from bubble’s interior until all that remains is pure argon. The theory is based on the fact that, at the elevated temperatures and pressures inside the bubble, dissociation of O_2 and N_2 into radicals is possible. These species then react with the water vapor radicals to form species that are soluble in the host fluid. As the pressure becomes very large during the compression stage of SBSL, the soluble materials leave the bubble and do not re-enter since their solubility in water is enormous compared to the Ar content of the bubble [48]. Over many cycles, the contents of an air bubble in water become nearly pure argon. Moreover, it was hypothesized that the SL would much more intense when the contents of the bubble are a pure inert gas: if the contents were e.g. molecules, bond breaking/formation would alter the pressure of the gas, ultimately reducing the temperature and reducing the amount of light production [5; 9; 10; 14]. This mechanism has been used to explain the relatively weak light, i.e. the low temperature, in MBSL: the bubbles are transient and cannot remove a significant amount of O_2 or N_2 over a single cycle. The current belief is that the contents of a bubble undergoing SBSL in water are pure argon after $\sim 10^3$ cycles [5; 14].

Still, most studies continued to use water as the host liquid until it was realized that SBSL in aqueous H_2SO_4 produces light 10^3 times brighter than in water, allowing more precise measurements of the light spectrum []. More importantly, new measurements revealed the phase space of SBSL in aqueous H_2SO_4 included a much larger range of pressure than water. Careful experiments revealed that the spectrum depended critically on the noble gas content and driving pressure. Suslick et. al measured the different emission spectra from Ar, Xe, and Kr bubbles in aqueous H_2SO_4 , driven to have similar conditions to those in an air bubble in water [10; 18; 19]. Importantly, they were able to identify spectral lines from Ar^+ , Xe^+ , and Kr^+ excited state transitions, proving that the core of the bubble is plasma. Perhaps equally as crucially, they found the *absence* of emission lines from components of aqueous H_2SO_4 vapor [10; 19; 19]: the plasma contained only the noble gas, experimentally confirming the argon rectification hypothesis. Moreover, the spectra at different pressures were in very good agreement with detailed calculations of emission from noble gas plasmas [15; 16]. Increased pressure results in increased collision rate between particles, broadening the excited state transition spectral lines [10; 16; 18; 19]. Further calculations showed that the greatly increased viscosity and density of aqueous H_2SO_4 , $\sim 10\times$ and $\sim 1.3\times$ larger than that of water, lead to reduced (by orders of magnitude) pressure in the bubble at the same driving pressures [15]. The larger pressure in the bubbles in water was found to be consistent with the featureless emission spectrum [10; 14].

This argon rectification hypothesis greatly helped to refine models for the gas dynamics in the bubble and clarified several unexplained experimental observations [5; 10]. With this in mind, we choose only to focus on results known to be relevant to the dynamics of a bubble undergoing SBSL. Excellent books and modern reviews on modeling the gas dynamics exist elsewhere [5; 14; 34]. We will hold off on discussing the dynamics in the plasma until a later section.

C. Gas Dynamics

The most straightforward way to model the gas dynamics in the bubble is through direct solution of the Navier-Stokes equations for the gas [5]. In fact, serious quantitative predictions of the conditions of the bubble’s interior take this path [15; 16; 17; 18; 19]. With simplifying assumptions, equations of motion with varying degrees of sophistication can be derived for the gas and the system of gas dynamical equations and the RP equations are solved numerically. The discussion proceeds in much the same way as deriving the RP equations above but is considerably more complicated [5; 14], so we will omit it here. An important aspect of these studies is the understanding of why relatively simple models work quite well. We will highlight the salient features before introducing a simple model for the gas that will enable us to gain some physical understanding analytically. An especially important result of direct numerical solution of the gas dynamics was (theoretical) confirmation of the argon rectification hypothesis [], reducing the possible gas dynamical models to those applicable to a monatomic gas. Various other models fully including dissipation and heat transport into/out of the bubble showed that the bubble’s compression is, to a good approximation, adiabatic and quasistatic []. Before we turn to discuss a model for the gas dynamics, let us pause to mention that another theoretically appealing method for modeling the gas dynamics is *molecular dynamics* []. While

this method is attractive for a number of reasons, practical calculations containing realistic numbers of particles aren't possible, limiting the applicability [5].

A simple but reasonable model for the gas dynamics in the bubble is that of an adiabatically, quasistatically compressed ideal gas [5]¹⁴. Let us remind ourselves what the pressure is in this case. Suppose that we have a volume, V , of an ideal gas containing N particles at a temperature T . The ideal gas law tells us the equation of state is $PV = Nk_B T$ with k_B *Boltzmann's constant*. Since we are assuming adiabatic compression, the second law of thermodynamics tells us that $dU = -PdV$ with U the internal energy in the gas. Moreover, we may use the equipartition theorem to write $dU = Nfk_B dT/2$ with f the number of *degrees of freedom* per particle []. Recall that for an ideal gas []:

$$\begin{aligned} C_V &= \frac{Nfk_B}{2} \\ C_P &= C_V + Nk_B \\ \frac{C_P}{C_V} &= 1 + \frac{2}{f} \equiv \gamma \end{aligned} \tag{14}$$

with C_V and C_P the heat capacities at constant volume and pressure respectively. For a monatomic ideal gas, $f = 3$ and $\gamma = 5/3$. Now we can use the second law of thermodynamics to write $C_V dT = -PdV$. From the equation of state, we have

$$dT = \frac{PdV + VdP}{Nk_B} = \frac{PdV + VdP}{C_P - C_V}. \tag{15}$$

Eliminating dT and simplifying,

$$\frac{dP}{P} = - \left(\frac{C_P}{C_V} \right) \frac{dV}{V} = -\gamma \frac{dV}{V}. \tag{16}$$

Integrating eq. 16, we find

$$P_2 = P_1 \left(\frac{V_1}{V_2} \right)^\gamma \tag{17}$$

where P_2 is the pressure in a gas at volume V_2 that was initially contained in a volume V_1 at pressure P_1 . Importantly we have not made any assumptions about the shape of the container.

Let us now connect this to the problem of SBSL. In our case, we assume that our bubble has an *ambient* radius R_0 where the pressure is at its equilibrium value, p_0 . The volume occupied by the gas is $V_0 = 4/3\pi R_0^3$. We know that $p_0 = p_\infty + 2\sigma/R$ from earlier. What we want to calculate is the pressure in the gas as a function of the bubble's instantaneous radius $R(t)$ determined from the RP equations (eq. 11 or eq. 13). Earlier we called the pressure in the gas $p_g(t)$ and we will stick with this here. Plugging these into eq. 17, (and sneaking in a modification) we arrive at a very commonly used equation in the context of SBSL [5; 27; 43; 44; 50]:

$$p_g(t) = \left(p_\infty + 2\frac{\sigma}{R_0} \right) \left[\frac{R_0^3 - h^3}{R^3(t) - h^3} \right]^\gamma \tag{18}$$

The new variable h that was added willy-nilly is called the *Van der Walls hard-core radius* and its purpose is to make sure that, if the bubble collapses so strongly that its contents become incompressible (i.e. $R(t) \rightarrow h$), the pressure diverges [5; 50]. Eq. 18 can be inserted into an RP equation which can then be integrated numerically to determine the bubble's dynamics.

Our physical intuition tells us why eq. 18 is sensible during the bubble's collapse: the bubble wall's velocity is fast and very little heat can flow out during compression. Detailed calculations starting from the full NS equations further tell us that the gas dynamics in the bubble can be regarded as *quasistatic* []. During the expansion and after-bounce stages of the bubbles cycle, which comprise its majority, the gas dynamics should instead be regarded as *isothermal*. This is true because, when the bubble's velocity is on the order of the *heat diffusion* timescale, the temperature

¹⁴ Actually we want to study a *Van der Walls* gas, but we will sneak this aspect in later. The modifications to the result for an ideal gas are simple [49].

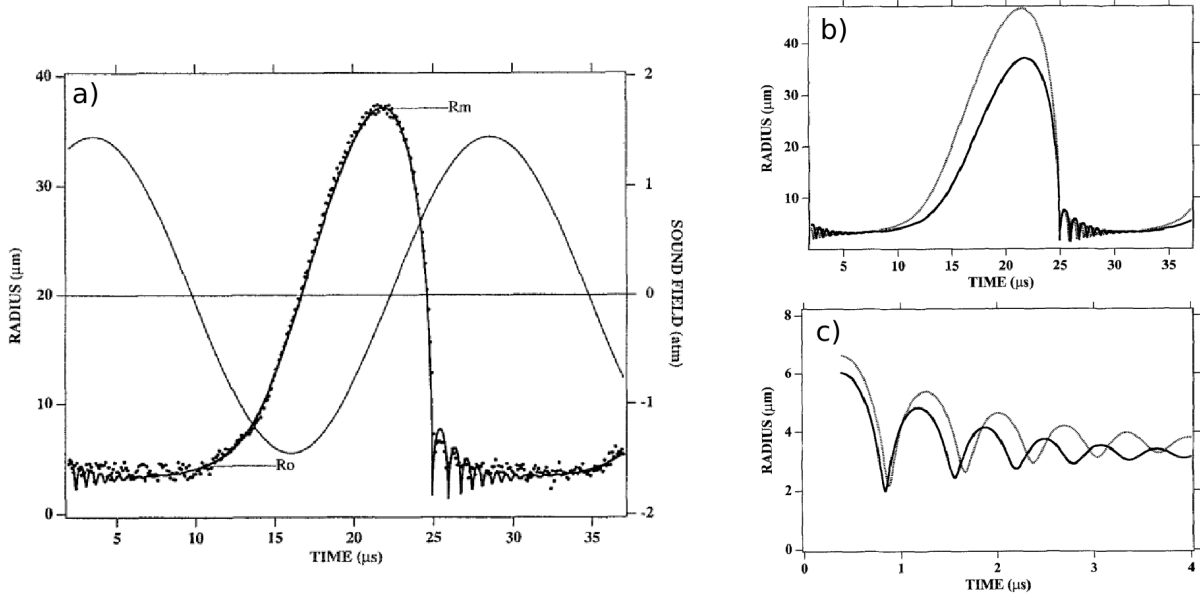


FIG. 5 [43; 51]

throughout the bubble is nearly equal to that in the liquid [5; 14; 26]. The relevant modifications to eq. 18 turns out to be replacing $\gamma \rightarrow 1$. A neat way of including both isothermal and adiabatic gas dynamics is continuously varying the exponent, γ in eq. 18, between its adiabatic and isothermal values, C_P/C_V and 1, respectively. A summary of this work is given in refs. [5] and [26]. It turns out that this process doesn't result in better quantitative predictions since, during the assumed isothermal part of the process, dissipation becomes important [5]. A simple alternative is choosing a constant exponent somewhere between the adiabatic $\gamma = 5/3$ and isothermal $\gamma = 1$ values [44]. It is also possible to include heat and mass diffusion in simple model forms and these do give slightly improved quantitative agreement with experiment; however we choose to discuss solutions of the RP equations using the simpler form given in eq. 18 as this will enable to understand the important features of the bubble's cycle. More advanced solutions using the full gas dynamical equations are qualitatively similar [5; 14].

Now recall that one of main goals of modeling the bubble dynamics in SBSL was to calculate the temperature inside the bubble in order to model the light emission. Following similar steps to deriving $p_g(t)$, we can write down an equation for the temperature T [5; 43]:

$$T(t) = T_0 \left(\frac{R_0^3 - h^3}{R^3(t) - h^3} \right)^{\gamma-1}. \quad (19)$$

Earlier, we assumed that during the bubble's after-bounces and expansion, the gas dynamics were isothermal. Then we take T_0 to be the temperature of the liquid. The RP equation, eq. 13, combined with the gas dynamical equation, eq. 18, and the known liquid and gas properties η , σ , and h , can be used to calculate the dynamics of an acoustically driven bubble, determining the time-dependence of the pressure and temperature in the bubble along the way.

D. Bubbles in the Lab

Creating stable, single bubbles in a laboratory experiment is not particularly challenging and can be done with standard and low-cost materials ¹⁵. A typical experimental setup is shown in Fig. 3. Since we are mainly concerned with the explaining the light emission process itself, we will only sketch the experimental setup; it can be summarized as follows [5; 7; 8; 10; 14; 22; 34; 52]. A sample of degassed liquid is placed into a flask ¹⁶. Coupled to the outside of

¹⁵ Actually, the phase-space for SBSL is "small". The coordinates being driving amplitude, driving frequency, fluid composition, temperature, ambient pressure, gas content and composition, etc... What we are claiming is simple is the experimental setup once the correct parameters are identified.

¹⁶ Actually, the degassing part is quite important. We focus on it elsewhere.

the flask are piezoelectric transducers of some sort. The piezos are driven by a sinusoidal function generator to excite an acoustic resonance of the flask: a typical flask is a few cm across with a resonance at ≈ 20 kHz [5]. The frequency is chosen to form a pressure *antinode* at the center of the flask.

Let us take a brief aside: in deriving the RP equations, we assumed the center of the bubble was stationary. Actually, this is what we want in an SBSL experiment and it is worth discussing under what conditions this is true. In an ideal, incompressible fluid the net force acting on a bubble may be written as

$$\mathbf{f} = - \int_{\partial\Omega} p \mathbf{n} dA = - \int_{\Omega} \nabla p dV \quad (20)$$

Here, \mathbf{f} is the net force, p is the pressure at the bubble's surface, \mathbf{n} is the unit normal vector point out of the bubbles surface, and $\partial\Omega$ is the bubble's boundary with Ω the bubble's domain. The last term is due to an application of Gauss's theorem. Bjerknes [53] took $\nabla p \equiv \nabla p(r=0, t)$ to be constant and averaged over one period of oscillation to find

$$\mathbf{f} = -\frac{4}{3}\pi \langle R^3 \nabla p \rangle. \quad (21)$$

This is the so called *Bjerknes force*. The point is that if the bubble is located at a pressure extrema, e.g. the antinode at the center of the flask, then this force should vanish and the bubble will remain stationary, an essential result for SBSL experiments.

Some authors have looked at corrections to the bubble's dynamics in the presence of buoyancy, which cause translational motion even for vanishing Bjerknes force. The result is the bubble oscillates around an equilibrium position near but away from the center of the flask [54; 55; 56]. The translational motion of the bubble leads to shape distortion which is believed to suppress SL; this is confirmed by SBSL experiments in microgravity resulting in larger intensity light production [54].

Back to the experimental setup. The typical driving pressure relevant to SBSL (~ 1.5 atm) is too small to cause bubbles to form spontaneously in the flask []. Instead, the bubble is usually seeded somehow. In the original work of Gaitan, an air bubble was injected using a needle and syringe through a small hole in the flask's seal [7]. More recently, seeding methods involve shooting a small jet of water into the flask (like our shrimp friends!) or blasting the water with a laser to boil a small volume []. The later method is preferred as it enables more precise control over the initial bubble's radius. The small bubbles formed this way coalesce at the center of the flask into a single, stable bubble [].

Now that we know about how single, stable bubbles are formed in the lab, we can discuss two experimentally accessible quantities that have turned out to be the most important: (i) The bubble's radius may be measured by *Mie scattering* and compared directly to solutions of the RP equations []. This can tell us about the temperature and pressure in the bubble. (ii) The other quantity of interest is the light spectrum which contains information on the bubble's contents: in principle, we can learn about temperature and pressure inside the bubble, with spectral lines telling us about the matter content []. As we will see, it is not simple to understand the light spectrum [] and we will devote a section of this paper to this topic. For now, let us see what measurements of the bubble's dynamics have told us.

Mie scattering measurements scatter a laser off a bubble and analyze the scattered intensity. Assuming the bubble is a homogeneous dielectric sphere [], the angular distribution of light scattered from the bubble at *fixed radius* and the time-dependent scattering off the bubble at *fixed angle* allow use to accurately measure the bubble's radius as a function of time []. A typical Mie scattering experiment is shown in fig. 3 (c). Two important sources of experimental error are changes to the dielectric properties of the bubble during its cycle [] and the fact that cavitating bubbles can emit an outward going shock []: some light scatters off the outward-going spherical wave too []. Both effects are largest during the SL period of the bubble's cycle, leading to an important source of error when fitting the calculated $R(t)$ curve []. Parameters used to calculate the gas dynamics in the bubble can then be fit to the measured radius to build a full model of the dynamics. In the case of eq. 18, the quantity to fit is R_0 . The results of a calculation using eq. 18 combined with the RP variant eq. 13 and fit to experiment are shown in fig. 5 (a). The ambient ambient radius is $R_0 = 1.45 \mu\text{m}$ for driving pressure $P_0 = 1.45$ atm [43; 51]. Note the large change in the calculated dynamics for relatively small changes in R_0 and P_0 in Fig. 5 (b) and (c).

More accurate treatments of the gas dynamics from numerically solving the gas's NS equations are qualitatively in good agreement with these simpler model calculations [5; 14]. They are, however, in better quantitative agreement when their results are used to calculate the light spectrum [10; 15; 16; 17; 18; 19]. Let us turn to discuss the light's spectrum now.

III. LET THERE BE LIGHT!

An important requirement for models of the light emission is *local thermodynamic equilibrium* (LTE). LTE is required for many reasons, foremost being the definition of temperature. LTE is expected to be true in a bubble undergoing SBSL since the particle density, $\sim 10^{28}/m^3$, and temperature, $\sim 10^4$ K, guarantee collisions between particles occur so frequently that equilibrium is ensured [5; 45; 57].

Any ensemble of atoms at a well defined temperature will emit radiation according to Planck's law. In the case of SBSL, we will look for corrections due to interactions of the emitted photons with atoms on the way out of the bubble [45]. Since we are assuming LTE, the intensity of emitted radiation depends instantaneously on the temperature-time curve, $T(t)$, that we calculated before. Planck's law is [58]

$$I_B(\lambda; T(t)) = \frac{2hc^2}{\lambda^5} \frac{1}{\exp(hc/\lambda k_B T(t)) - 1} \quad (22)$$

The *black-body model* assumes the bubble is optically thick and that all radiation emitted inside the bubble is absorbed on its way out. Then the only emission that is measured comes from a thin layer on the bubble's surface. Calculations of SBSL assuming this over-estimate the number of photons emitted by orders of magnitude [5; 44]. Instead, we need to consider finite opacity of the bubble, i.e. some of the emitted radiation is absorbed on its way out.

Let's call the absorption coefficient $\kappa(\lambda, T(t))$ ¹⁷ where we allow dependence on both wavelength λ and temperature, $T(t)$. Then the intensity of light that has travelled a distance s through the bubble is denoted by [59]

$$I(\lambda; T(t)) = I_B(\lambda; T(t)) (1 - \exp[-\kappa(\lambda; T(t))s]) \quad (23)$$

where we have continued with the approximation that the temperature in the bubble is uniform [44; 45]. In the limit that $\kappa \rightarrow \infty$, we recover the result for a black-body emitter. On the other hand, for a strong absorber, $1 - \exp(\kappa s) \approx \kappa s$ and $I \approx I_B \kappa s$, i.e. the number of photons emitted is greatly reduced, a result that we require. For more complicated $\kappa(\lambda; T(t))$ that may even depend on *position* through $T(\mathbf{x}, t)$ in a more accurate gas dynamical model, eq. 23 is integrated numerically. Moreover, integrating over the bubble's volume and surface, and over time, allow calculating the radiated power spectrum which may be directly compared to experiment. A great deal of work has been devoted to identifying the relevant absorption mechanisms, with most progress being made only after SBSL was discovered in aqueous H_2SO_4 [5; 10; 15; 16; 17; 18; 19; 44; 45; 57].

What was discovered is that the radiative processes occurring during SBSL depend very sensitively on the fluid properties and driving pressure [18; 19]. Due to its different mechanical properties, H_2SO_4 can support SBSL over a larger range of driving pressures than water [15]. For low driving pressures, the temperature and pressure in the bubble are much lower than those encountered in bubbles in water and *discrete* emission lines for molecular dissociation and electronic transitions are directly observable [18; 19]. At larger driving pressures leading to bubble conditions comparable to those in water, however, what was found is that the *continuous* processes electron-ion bremsstrahlung, electron-atom bremsstrahlung, and electron-ion recombination dominate [10; 14; 44; 59]. Moreover, it is now known that radiative (de)attachment of electrons and water-vapor molecules for SBSL in water is an important source of absorption, though this effect is limited by the small amount of these species in the bubble (see the argon rectification hypothesis above) [17].

Let us discuss SBSL of a *pure* Ar bubble in water. At the very high temperatures that occur in the bubble, a large fraction of (outer-shell) electrons are in excited states or are ionized from their atoms completely [59]. Moreover, at the very high temperature and pressures in the bubble ($\sim 10^4$ K, \sim GPa), collisions between the particles are frequent. When an ionized electron passes near an atom or (not so near) an ion, it is deflected by the atom's potential. The deflection accelerates the electron, changing its kinetic energy. Since mass of the ion or atom is much greater than the mass of the electron, we can take the atom or ion to be fixed. Since the electron is charged (and energy is conserved), it emits radiation through *bremsstrahlung* as its kinetic energy changes [36; 59]. It is also possible for the electron to become *bound* to the ion, emitting light to lower its kinetic energy.

The *Saha equation* of astrophysics allows us to estimate the fraction of particles that are ionized at a given temperature [17; 44; 59]

$$\alpha(T(t)) \approx \left(\frac{2\pi m_e k_B T}{h^2} \right)^{3/4} \exp \left(-\frac{E_{ion}}{2k_B T} \right) \quad (24)$$

¹⁷ Really, this is an *effective* absorption coefficient $\kappa = \kappa'(1 - \exp[-hc/k_B T \lambda])$ with κ' the actual absorption coefficient of the material. The effective coefficient κ includes induced emission of photons as light passes through the medium which 'decreases' absorption. Physically, this can be viewed as radiation that is absorbed being immediately re-emitted or, equivalently, vice-versa [59; 60].

It turns out that at typical SBSL temperatures, only $\sim 1\%$ of the atoms are ionized and thus, since collisions are very frequent, electron-neutral atom bremsstrahlung is perhaps as important as electron-ion processes [17; 18; 44]. For Ar^+ and e , formulas for recombination and electron-ion bremsstrahlung can be found in ref. [44]. For electron-atom processes, most modern work follows that of Geltman [16; 17; 61].

For electron-ion collision, the potential leading to bremsstrahlung is the long range Coulomb interaction and analytical calculations are available. For electron-atom collision, the potential is short range and the emission is very sensitive to the potential. The best route is numerical calculations with pseudopotentials [61].

Book [59] gives a very good heuristic explanation of the the absorptions processes in III.2. Also interesting: "Let us imagine an infinite medium in thermodynamic equilibrium at a constant temperature T . Under steady state conditions the radiation field will also be in equilibrium. Thermal radiative equilibrium is characterized by the fact that the number of photons or amount of radiant energy emitted by the medium per unit time per unit volume in a given frequency interval $d\nu$ and in a given differential solid angle $d\Omega$ is exactly equal to the number of absorbed photons or to the radiant energy absorbed by the medium in the same intervals $d\nu$ and $d\Omega$." Also "Kirchhoff's law expresses the general principle of detailed balancing applied to the emission and absorption of light. It allows us to calculate the emission coefficient of a substance if the absorption coefficient is known (and vice versa)."

Gives the three important processes: (i) free-free transitions such as electron-ion and electron-atom *bremsstrahlung*. (ii) bound-free transitions such as detachment/recombination of electrons and ions, and (iii) bound-bound transitions such as transitions between bound electronic states in an atom. Both (i) and (ii) produce continuous spectra, while (iii) leads to *lines* [59].

Early work ignored bound-bound transitions since lines weren't observed in spectrum. Argued that they would be very broad, but estimated the broadening was too small to lead to what was seen in experiment, concluding instead that these process don't occur and that the relevant species aren't present in the bubble [44; 45]. Later work used more accurate gas dynamical models to show which species are important [16; 17; 17] and, when correctly including the broadening, pretty much all features of the spectra in water and aqueous H_2SO_4 are predicted correctly [10; 18; 19].

IV. SUMMARY

V. ACKNOWLEDGMENTS

Appendix A: The Navier-Stokes Equation

The Rayleigh-Plesset (RP) equation can be deduced from the Navier-Stokes equations [5; 10; 14; 25; 26; 33]. To that end, we remind ourselves of the Navier-Stokes equations here.

The *total* change (in time) of mass in an arbitrary element of a fluid (whose coordinates and boundary may depend on time) is given by $\frac{d}{dt} \int_{\Omega_t} \rho dV$ where Ω_t is the domain of the fluid element under consideration and $\rho(\mathbf{x}, t)$ is the local, time-dependent density of the fluid. Using the transport theorem of fluid dynamics [62], Gauss's theorem, and (with only some loss of generality) taking Ω_t to be a *fluid parcel* (so that the boundary of the fluid parcel, $\partial\Omega_t$, moves with the fluid's velocity, $\mathbf{u}(\mathbf{x}, t)$), this becomes

$$\frac{d}{dt} \int_{\Omega_t} \rho dV = \int_{\Omega_t} \partial_t \rho dV + \int_{\partial\Omega_t} \rho \mathbf{u} \cdot \mathbf{n} dA = \int_{\Omega_t} \partial_t \rho + \nabla \cdot (\rho \mathbf{u}) dV. \quad (\text{A1})$$

Now to have *mass-continuity*, which we will require on physical grounds, we set eq. A1 to 0. Basically, we are saying no additional material is being added or removed from the fluid. Since the fluid parcel's boundary Ω_t is arbitrary, we find that $\partial_t \rho + \nabla \cdot (\rho \mathbf{u}) \equiv 0$ which is true for every point in the fluid volume.

Newton's second law for fluids (*momentum-continuity*) is defined similarly [62; 63]. We write the momentum-density as $\rho \mathbf{u}$ with momentum given by $\int_{\Omega_t} \rho \mathbf{u} dV$. To simplify what follows, we focus on only the i^{th} component of velocity at a time. Then Newton's second law can be written as

$$\frac{d}{dt} \int_{\Omega_t} \rho u_i dV = \int_{\Omega_t} \partial_t (\rho u_i) dV + \int_{\partial\Omega_t} \rho u_i (\mathbf{u} \cdot \mathbf{n}) dA = F_i. \quad (\text{A2})$$

Now using Gauss's theorem, the product rule, and mass-continuity we find $\frac{d}{dt} \int_{\Omega_t} \rho u_i dV = \int_{\Omega_t} \rho \frac{du_i}{dt} dV = F_i$. In vector notation this reads

$$\int_{\Omega_t} \rho \frac{d\mathbf{u}}{dt} = \mathbf{F} \quad (\text{A3})$$

We now turn to the forces. Let us separate the forces into *body-* and *surface-forces*: $\mathbf{F} = \int_{\Omega_t} \mathbf{f}_B dV + \int_{\partial\Omega_t} \mathbf{f}_S dA$. The body-force density, \mathbf{f}_B , is due to forces acting in the bulk of the liquid e.g. gravity, electrostatic forces, etc. and is typically from sources external to the liquid. We won't be concerned with these forces here. Instead, let us concentrate on the surface part. If we only consider an ideal fluid, the surface part can be written as $\int_{\partial\Omega_t} \mathbf{f}_S dA = - \int_{\partial\Omega_t} p \mathbf{n} dA = - \int_{\Omega_t} \nabla p dV$ with p the pressure and the minus sign being due to the sign convention: *out* of the surface $\partial\Omega_t$ is positive.

If instead the fluid is real, we can't neglect viscous forces. We suppose that the viscous surface term can be represented by a tensor, $\hat{\boldsymbol{\tau}}$ such that $\mathbf{F}_v = \int_{\partial\Omega_t} \hat{\boldsymbol{\tau}} \cdot \mathbf{n} dA = \int_{\Omega_t} \nabla \cdot \hat{\boldsymbol{\tau}} dV$. (Note, here the dot product is to be understood as matrix multiplication). To leading order in gradients of the velocity, (and under the physical constraints that the tensor be symmetric), the viscous-stress tensor is $\hat{\boldsymbol{\tau}} = \hat{\boldsymbol{\mu}} \cdot \hat{\boldsymbol{\epsilon}}$ where $\hat{\boldsymbol{\mu}}$ is the viscosity-tensor and $\hat{\boldsymbol{\epsilon}}$ is the strain-rate tensor: $\epsilon_{ij} = \frac{1}{2} [\partial_i u_j + \partial_j u_i]$.

In general, $\hat{\boldsymbol{\mu}}$ is a symmetric rank-4 tensor. However, if we assume an isotropic fluid¹⁸, we find that the viscous-stress tensor can be separated into two irreducible parts: a scalar, $\hat{\boldsymbol{\epsilon}}^{(v)}$, and traceless symmetric part, $\hat{\boldsymbol{\epsilon}}^{(s)}$ [64; 65]:

$$\begin{aligned}\hat{\boldsymbol{\tau}} &= \xi \hat{\boldsymbol{\epsilon}}^{(v)} + \mu \hat{\boldsymbol{\epsilon}}^{(s)} \\ \hat{\boldsymbol{\epsilon}}^{(v)} &= \delta_{ij} \epsilon_{kk} \\ \hat{\boldsymbol{\epsilon}}^{(s)} &= \hat{\boldsymbol{\epsilon}} - \frac{1}{3} \delta_{ij} \epsilon_{kk}.\end{aligned}\tag{A4}$$

Thus, we see that the viscosity-tensor only has two free components: ξ , the normal viscosity and μ the shear viscosity. It is usual to combine the pressure (i.e. elastic-stresses) and the viscous-stresses into the stress-tensor $\hat{\boldsymbol{\sigma}} = -p \hat{\mathbf{I}} + \xi \hat{\boldsymbol{\epsilon}}^{(v)} + \mu \hat{\boldsymbol{\epsilon}}^{(s)}$. Combined with this, Newton's second law becomes

$$\int_{\Omega_t} \rho \frac{d\mathbf{u}}{dt} - \mathbf{F} = \int_{\Omega_t} \rho \frac{d\mathbf{u}}{dt} - \nabla \cdot \hat{\boldsymbol{\sigma}} - \mathbf{f}_B dV = 0\tag{A5}$$

Again, since we allow the volume of integration to be arbitrary, the integrand must vanish everywhere: $\rho \frac{d\mathbf{u}}{dt} - \nabla \cdot \hat{\boldsymbol{\sigma}} - \mathbf{f}_B = 0$. This is the momentum-continuity equation for a fluid. Now we would rather have this explicitly in terms of the velocity \mathbf{u} . To that end, we may substitute eq. A4 into the momentum-continuity equation. For e.g. the i^{th} component we may expand out the divergence part as

$$(\nabla \cdot \hat{\boldsymbol{\sigma}})_i = -\partial_i p + \left[\xi + \frac{2}{3} \mu \right] \partial_i (\nabla \cdot \mathbf{u}) + \mu \nabla^2 u_i \equiv -\partial_i p + \eta \partial_i (\nabla \cdot \mathbf{u}) + \mu \nabla^2 u_i\tag{A6}$$

where we have introduced the *bulk-viscosity* $\eta = \xi + \frac{2}{3} \mu$. Collecting all of the components into vector form and, combined with the mass-continuity equation A1, we arrive at the *Navier-Stokes* (NS) equations for a compressible fluid:

$$\begin{aligned}\rho \frac{d\mathbf{u}}{dt} &= \rho [\partial_t \mathbf{u} + (\mathbf{u} \cdot \nabla) \mathbf{u}] = -\nabla p + \eta \nabla (\nabla \cdot \mathbf{u}) + \mu \nabla^2 \mathbf{u} + \mathbf{f}_B \\ \partial_t \rho + \nabla \cdot (\rho \mathbf{u}) &= 0.\end{aligned}\tag{A7}$$

Some comments are in order. The total-derivative of a moving fluid $\frac{d}{dt} \equiv D_t$ is sometimes called the *material derivative*. In the case of velocity $D_t \mathbf{u}$ is the *acceleration* of the fluid. It records not only explicit time dependence of the fluid's velocity $\partial_t \mathbf{u}$ but also how the fluid's velocity varies *in space* as it moves past us: $(\mathbf{u} \cdot \nabla) \mathbf{u}$. The pressure term on the right hand side is to be understood as forces from the *elastic* energy. On the other hand, the terms $\sim \mathbf{u}$ are viscous terms that tend to make the velocity field spatially uniform: they vanish when the (spatial) derivatives of the velocity vanish. The bulk-viscosity term $\sim \eta$ damps radial changes in the fluids velocity (e.g. dilation/contraction) while the shear-viscosity term $\sim \mu$ resists shearing. The body term \mathbf{f}_B is from external sources. It is worth noting that solving eqs. A7 is a formidable task¹⁹ and is usually done using computers.

¹⁸ Definitely true for water which has been frequently used in SL experiments.

¹⁹ In fact, it's not even clear that the NS equations *can* be solved even for incompressible fluids. In 2000, it was announced that proving smooth, sensible solutions exist earns \$1,000,000 [66]. Better hurry though... inflation was 6.8% in Nov. 2021.

Appendix B: Electrical Arguments

Appendix C: The Casimir Argument

REFERENCES

- [1] M. Versluis, B. Schmitz, A. Von der Heydt, and D. Lohse, *Science* **289**, 2114 (2000).
- [2] D. Lohse, B. Schmitz, and M. Versluis, *Nature* **413**, 477 (2001).
- [3] X. Tang and D. Staack, *Science advances* **5**, eaau7765 (2019).
- [4] F. A. Everest, R. W. Young, and M. W. Johnson, *The Journal of the Acoustical Society of America* **20**, 137 (1948).
- [5] M. P. Brenner, S. Hilgenfeldt, and D. Lohse, *Reviews of modern physics* **74**, 425 (2002).
- [6] L. A. Crum and R. A. Roy, *Science* **266**, 233 (1994).
- [7] D. F. Gaitan, L. A. Crum, C. C. Church, and R. A. Roy, *The Journal of the Acoustical Society of America* **91**, 3166 (1992).
- [8] D. F. Gaitan, *An experimental investigation of acoustic cavitation in gaseous liquids*, Ph.D. thesis, The University of Mississippi (1990).
- [9] D. Lohse, *Physical review fluids* **3**, 110504 (2018).
- [10] K. S. Suslick and D. J. Flannigan, *Annu. Rev. Phys. Chem.* **59**, 659 (2008).
- [11] J. Schwinger, *Proceedings of the National Academy of Sciences* **90**, 958 (1993).
- [12] C. Eberlein, *Physical Review Letters* **76**, 3842 (1996).
- [13] S. Liberati, M. Visser, F. Belgiorno, and D. Sciama, *Journal of Physics A: Mathematical and General* **33**, 2251 (2000).
- [14] K. Yasui, *Acoustic cavitation and bubble dynamics* (Springer, 2018).
- [15] Y. An and C. Li, *Physical Review E* **80**, 046320 (2009).
- [16] Y. An and C. Li, *Physical Review E* **78**, 046313 (2008).
- [17] Y. An, *Physical Review E* **74**, 026304 (2006).
- [18] D. J. Flannigan and K. S. Suslick, *Nature* **434**, 52 (2005).
- [19] D. J. Flannigan, S. D. Hopkins, C. G. Camara, S. J. Putterman, and K. S. Suslick, *Physical review letters* **96**, 204301 (2006).
- [20] N. Marinesco and J. Trillat, *Proceedings of the Royal Academy of Science* **196**, 858 (1933).
- [21] H. Frenzel and H. Schultes, *Zeitschrift für Physikalische Chemie* **27**, 421 (1934).
- [22] B. Gompf and R. Pecha, *Physical Review E* **61**, 5253 (2000).
- [23] S. Li, C. E. Brennen, and Y. Matsumoto, *Introduction for amazing (cavitation) bubbles* (2015).
- [24] L. Rayleigh, *On the pressure developed in a liquid during the collapse of a spherical cavity: Philosophical magazine series* **6**, 34, 94–98 (1917).
- [25] M. S. Plesset and A. Prosperetti, *Annual review of fluid mechanics* **9**, 145 (1977).
- [26] A. Prosperetti, *Sonochemistry and sonoluminescence* , 39 (1999).
- [27] R. Löfstedt, K. Weninger, S. Putterman, and B. P. Barber, *Physical Review E* **51**, 4400 (1995).
- [28] B. P. Barber, R. Hiller, K. Arisaka, H. Fetterman, and S. Putterman, *The Journal of the Acoustical Society of America* **91**, 3061 (1992).
- [29] B. P. Barber and S. J. Putterman, *Nature* **352**, 318 (1991).
- [30] C. Wu and P. H. Roberts, *Physical review letters* **70**, 3424 (1993).
- [31] H. P. Greenspan and A. Nadim, *Physics of Fluids A: Fluid Dynamics* **5**, 1065 (1993).
- [32] R. Hiller, S. J. Putterman, and B. P. Barber, *Physical review letters* **69**, 1182 (1992).
- [33] A. Prosperetti and A. Lezzi, *Journal of Fluid Mechanics* **168**, 457 (1986).
- [34] C. E. Brennen, *Cavitation and bubble dynamics* (Cambridge University Press, 2014).
- [35] M. S. Plesset, (1949).
- [36] J. D. Jackson, *Classical electrodynamics* (1999).
- [37] T. Leighton, (2007).
- [38] J. B. Keller and M. Miksis, *The Journal of the Acoustical Society of America* **68**, 628 (1980).
- [39] A. Lezzi and A. Prosperetti, *Journal of Fluid Mechanics* **185**, 289 (1987).
- [40] A. Prosperetti, L. A. Crum, and K. W. Commander, *The Journal of the Acoustical Society of America* **83**, 502 (1988).
- [41] J. B. Keller and I. I. Kolodner, *Journal of applied physics* **27**, 1152 (1956).
- [42] K. Yasui, in *Sonochemistry and the Acoustic Bubble* (Elsevier, 2015) pp. 41–83.
- [43] B. P. Barber, R. A. Hiller, R. Löfstedt, S. J. Putterman, and K. R. Weninger, *Physics Reports* **281**, 65 (1997).
- [44] S. Hilgenfeldt, S. Grossmann, and D. Lohse, *Nature* **398**, 402 (1999).
- [45] S. Hilgenfeldt, S. Grossmann, and D. Lohse, *Physics of fluids* **11**, 1318 (1999).
- [46] K. Weninger, R. Hiller, B. P. Barber, D. Lacoste, and S. J. Putterman, *The Journal of Physical Chemistry* **99**, 14195 (1995).
- [47] R. Hiller, K. Weninger, S. J. Putterman, and B. P. Barber, *Science* **266**, 248 (1994).
- [48] D. Lohse, M. P. Brenner, T. F. Dupont, S. Hilgenfeldt, and B. Johnston, *Physical review letters* **78**, 1359 (1997).
- [49] S. Sivasubramanian, A. Widom, and Y. Srivastava, *arXiv preprint cond-mat/0207465* (2002).
- [50] R. Löfstedt, B. P. Barber, and S. J. Putterman, *Physics of Fluids A: Fluid Dynamics* **5**, 2911 (1993).
- [51] B. P. Barber and S. J. Putterman, *Physical review letters* **69**, 3839 (1992).
- [52] W. Lentz, A. A. Atchley, and D. F. Gaitan, *Applied optics* **34**, 2648 (1995).

- [53] V. Bjerknes, *Die Kraftfelder*, Vol. 28 (F. Vieweg, 1909).
- [54] T. J. Matula, *Ultrasonics* **38**, 559 (2000).
- [55] T. J. Matula, S. M. Cordry, R. A. Roy, and L. A. Crum, *The Journal of the Acoustical Society of America* **102**, 1522 (1997).
- [56] T. J. Matula, *Philosophical Transactions of the Royal Society of London. Series A: Mathematical, Physical and Engineering Sciences* **357**, 225 (1999).
- [57] K. Yasui, *Physical review E* **60**, 1754 (1999).
- [58] D. V. Schroeder, *An introduction to thermal physics* (1999).
- [59] Y. B. Zel'Dovich and Y. P. Raizer, *Physics of shock waves and high-temperature hydrodynamic phenomena* (Courier Corporation, 2002).
- [60] R. L. Taylor and G. Caledonia, *Journal of Quantitative Spectroscopy and Radiative Transfer* **9**, 657 (1969).
- [61] S. Geltman, *Journal of Quantitative Spectroscopy and Radiative Transfer* **13**, 601 (1973).
- [62] J. M. McDonough, (2009).
- [63] L. Schoeffel, arXiv preprint arXiv:1407.3162 (2014).
- [64] A. Zee, *Group theory in a nutshell for physicists*, Vol. 17 (Princeton University Press, 2016).
- [65] L. Landau and E. Lifshitz, *Course of Theoretical Physics* **6** (1987).
- [66] C. L. Fefferman, *The millennium prize problems* **57**, 22 (2006).